Journal of Materials Science: Materials in Electronics (2020) 31:2557–2566
https://doi.org/10.1007/s10854-019-02793-w

Synthesis and characterization of La^{3+} ions incorporated (PVA/PVP) polymer composite films for optoelectronics devices

F. M. Ali[1,2] · **R. M. Kershi**[1,3]

Received: 24 October 2019 / Accepted: 19 December 2019 / Published online: 2 January 2020

Abstract
Polymer rare-earth composite films PVA/PVP–xLa^{3+} ($x$wt%; $x = 0$, 3, 5, 10, and 15) were fabricated by the solution casting method. The structural parameters of these films were determined from X-ray diffraction (XRD) pattern analysis, and the complexation of La^{3+} ions with the polymer composite films was studied by Fourier transform infrared (FT-IR) spectroscopy. The optical energy gap ($E_{opt.}$) and the high-frequency refractive index (n) were determined from UV–Vis transmission spectra analysis. AC electrical conductivity and dielectric characterization of the polymer composite films have been investigated. The structural parameters of the inter-planar (d) spacing, crystallite length (D), and the average crystallite separation (R) and the FT-IR spectra indicate strong bonding of La^{3+} ions with the carbonyl groups of the polymer composite chains. The optical gaps of the films determined by Tauc's relation and optical absorption fitting (ASF) exhibit a slight decrease by increasing La^{3+} ions content, whereas the refractive indices show a slight increase. High values of the dielectric parameter ε' and dielectric loss ε'' were produced in pure PVA/PVP composite polymer films, and they tend to decrease by increasing La^{3+} ions content in the PVA/PVP composite films due to decreasing directional polarization and ionic polarization in the films with increasing La^{3+} ions content. The minimum energy loss occurred at 70 kHz and these materials may be selected to be used in energy applications. I–V characteristics show a linear-like ohmic behavior because La ions are bonded well in the structure of polymers and became part of it.

1 Introduction

During the last two decades, development of inexpensive composite polymers with lightweight, good mechanical strength, desired optical, and electrical properties have received a lot of attentions from technical and academic researchers. These materials can be used as multifunctional materials in wide applications including industrials and optical technologies. Owing to the relatively large ion size, electrostatic interaction with the polar groups of polymeric materials, and their tendency to form covalent bonds, rare-earth elements (REEs) doping has considerable effects on the structural, optical, and thermal properties of many types of host polymer [1–3].

Among various polymers, polyvinyl alcohol (PVA) $(C_2H_4O)_n$ and polyvinyl pyrrolidone (PVP) $(C_6H_9ON)_n$ and their blend (PVA/PVP) have recently received considerable interest with numerous potential applications [3–9]. The properties of these polymers can be improved and controlled substantially by doping with rare-earth ions. Polyvinyl alcohol films can be used as a host matrix for appropriate dopant such as transition metal elements, rare-earth ions, and dyes, which can be used for wide range of applications as in image storage, holography, laser applications, sensors, photonic devices, and photovoltaic cells [3–11]. Its semi-crystalline structure showed an important feature where the semi-crystalline materials have exhibited improvement in certain physical properties due to crystalline–amorphous interfacial effect [11–15]. Some studies revealed that the optical and thermal properties of the PVA can be controlled by various doping materials for different applications [14–19]. PVP is a vinyl polymer amorphous polymer of high glass transition temperature (T_g) having a rigid pyrrolidone group in its structure that is responsible for excellent complexation with

✉ F. M. Ali
Fayezbakeer@yahoo.com

[1] Physics Department, Faculty of Science, King Khalid University, P. O. Box 9004, Abha 61413, Saudi Arabia

[2] Physics Department, Faculty of Science, Suez Canal University, Ismailia 41522, Egypt

[3] Physics Department, Faculty of Science, Ibb University, Ibb, Yemen

other polymers to form composites with good mechanical properties [3, 4, 18]. PVA and PVP are ecofriendly polymers easily soluble in water and having excellent film forming ability. The solution composed of PVA and PVP polymers is one of the low cost and available methods extensively used to get new material with improved properties useful for promising optical and electrical application [19–27].

The long-term stability, a water-soluble polymer, and ease of processing permit the use of PVA and PVP as a convenient host matrix for rare-earth ions (REIs). REIs in their trivalent state are partially filled 4f sub-shell [28, 29] and contain highly electronegativity donor atoms and PVA also possesses potential oxygen donors, therefore PVA/PVP composite can interact with rare-earth ions (REIs) to produce important structural and optical features [3, 4, 30, 31].

The main objective of the present study is to prepare 50PVA/50PVP per weight (wt%) doped with different weight percentages ($x$wt%; $x = 0$, 3, 5, 10, and 15) of $La(NO_3)_3{\cdot}6H_2O$ to study the influence of La^{3+} ions on the microstructural, optical, electrical, and dielectric characterization of the PVA/PVP composite. The prime novelty of this work is to develop and characterize low cost prepared polymer—rare-earth composite films aiming to enhance their optical properties and applications.

2 Experimental section

2.1 Samples preparation

Polymer films can be prepared by different methods such as melt pressing, melt extrusion, and solution casting techniques. Each technique has its own advantages and limitations. The melt pressing and melt extrusion are used in the preparation of films from the polymer melts. The primary drawback of these two techniques is subjecting the film constituents to high temperatures, which may cause thermal degradation. The solution casting technique has been paid significant attention due to its potential advantages such as thickness uniformity, good clarity, more flexibility, and better physical properties. This method is simple but it needs long time to ensure a complete solubility and homogeneity of the raw polymeric materials in their solvents. In this work, the solution casting technique is used for preparation of La^{3+}-doped PVA/PVP polymer blend composite films by solving the ingredients in distilled water.

The raw chemical materials of two polymers polyvinyl alcohol (PVA) of molecular weight (mw = 57,000–66,000 g/mol.), polyvinyl pyrrolidone (PVP) (mw = 58,000 g/mol.) and Lanthanum (III) nitrate hydrate [$La(NO_3)_3{\cdot}6H_2O$, (99.9%)] rare-earth salt used in the preparation of polymer composite films were supplied from Alfa Aesar Karlsruhe, Germany. Polymer blend composite films (PVA/PVP–$x$$La^{3+}$); $x = 0$, 3, 5, 10, and 15 per weight were prepared using the low-cost casting technique. Two equal weights of PVA and PVP were separately dissolved in fresh distilled water using magnetic stirrer for 8 h at 60 °C till obtaining homogenous and transparent solutions. The two solutions are then mixed together with subsequent stirring for 2 h. The polymer composite films PVA/PVP–$x$wt% $La(NO_3)_3{\cdot}6H_2O$ were prepared by mixing the required weight fraction (wt%) of the dopant to the polymer composite solutions. These solutions were stirred well to obtain homogenous mixtures which were then poured into perfectly flat petri dishes and left to dry at the ambient temperature for one weak to get free-standing films. The PVA/PVP–$x$$La^{3+}$; $x = 0$, 3, 5, 10, and 15 films were carefully peeled from the glass petridishes and coded as sample A, B, C, D, and E, respectively.

2.2 Characterization techniques

The X-ray diffraction patterns of pure and La^{3+} ions doped with PVA/PVP polymer composite were studied using Shimadzu model XRD-6000 X-ray Diffractometer in the Bragg's angle range of $5° \leq 2\theta \geq 60°$ and Cu K_α radiation of wavelength $\lambda = 1.5406$ Å with scanning speed of 5°/min. Thermo Nicolet 6700 FT-IR spectrometer was used to record the FT-IR spectra of the fabricated composite films in the wave number range 500–4000 cm^{-1} with a resolution of 4 cm^{-1}. JASCO (V-570-UV–Vis-NIR) spectrophotometer was used for the optical transmission and absorption measurements of the investigated films in the wavelength range of 200–800 nm. The dielectric characterization and AC conductivity of the samples were carried out by LCR bridge meter model Agilent 4284A Precision as a function of frequency in the range from 1.2 kHz to 1 MHz at room temperature. I–V characteristics were studied using two-probe experimental set-ups (Model DNM-121, SES Instruments Pvt. Ltd, Roorkee, India). Both sides of the investigated polymer film samples were precisely painted with silver paste electrodes and mounted on a designed sample holder that is used to study the dielectric and electrical properties of the prepared films.

3 Results and discussions

3.1 The structural parameters

Figure 1 shows the recorded XRD pattern of pure PVA/PVP and PVA/PVP–La^{3+} polymer composite films. It is noted from the Figure that (I) a relatively broad hump is observed at about $2\theta = 19.73°$ for pure PVA/PVP. This peak attributed to the (101) reflection plane of PVA which agrees well with various reported works [32–35] and confirms the miscibility

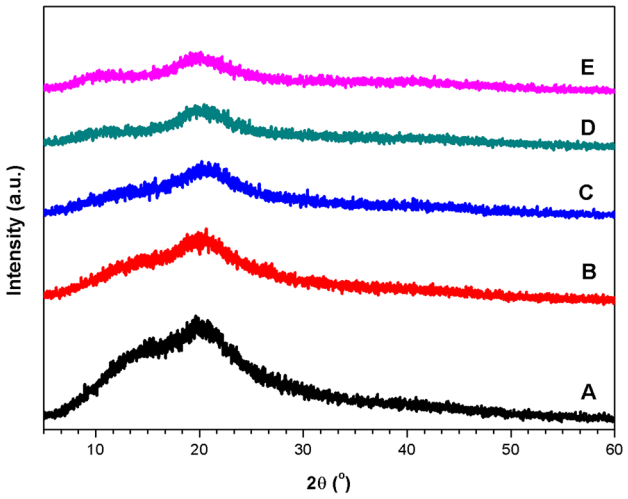

Fig. 1 XRD patterns of PVA/PVP–xLa^{3+} polymer composite films

of the two polymers due to strong interaction between the OH groups of the semi-crystalline PVA and the C=O of the amorphous PVP to form a composite film which contains amorphous and crystalline regions. (II) On doping the PVA/PVP composite with different concentrations of lanthanum salts, there are no additional peaks corresponding to the crystalline nature of the salt observed in the XRD patterns which indicates the complete dissociation and homogenous complexation of the salt in the polymer matrix through bonding of La^{3+} ions with the carbonyl group in the polymer composite chains. (III) It is interesting to note that, after doping, the intensity of the observed broad beak gets decreased; its position shifts slightly towards higher diffraction angle and exhibits reduction in FWHM (see Table 1). This result indicates incorporation of La^{3+} ions in the hybrid polymer composite film and implies an augmentation of the amorphous regions [32–36]. Various structural parameters such as the inter-planar spacing (d), the crystallite size (D), the relative intensity of the peak (I/I_o %), and the average crystallite separation (R) were determined form Bragg's angle θ and the FWHM of the Gaussian fitting of the main peak according to the following relations listed in References [32–37].

$$d = \frac{n\lambda}{2\sin\theta}, \tag{1}$$

$$D = \frac{0.94\lambda}{\beta\cos\theta}, \tag{2}$$

and

$$R = \frac{5\lambda}{8\sin\theta}, \tag{3}$$

respectively, where λ is the wavelength (1.5406 Å) of the X-ray radiation and $n = 1$ for the first-order diffraction. These parameters are listed in Table 1. For brevity, the Gaussian fittings of the main XRD peak for pure PVA/PVP and PVA/PVP–15wt%La^{3+} samples are shown in Fig. 2a and b, respectively.

It is noticed from Table 1 that, although the La^{+} ions content has a small effect on the (d) and (R) values of PVA/PVP–La^{3+}, a dramatic decrease on the relative intensity (I/I_o) peak occurred due to doping of the PVA/PVP polymer composite with low (3wt%) La^{3+} ions and this change becomes relatively small for the higher La^{3+} ions content. This means that small amount of rare-earth ions leads to a significant decrease in the degree of crystallinity of the polymer composite. It is interesting to note that doping PVA/PVP composite with La^{3+} ions leads to a slight decrement in the average inter-chain separation of the PVA/PVP–xLa^{3+} composite. Thus, incorporation of Lanthanum ions in the PVA/PVP composite film brought more compact structure of final composite due to the strong interaction of La^{3+} with the carbonyl groups of the PVA/PVP composite.

3.2 FT-IR spectroscopy analysis

It has been established that, FT-IR spectroscopy is a powerful technique to investigate and provides worthy knowledge about the structure and chemical species of the polymer composite films. The FT-IR transmission spectra for pure PVA/PVP and PVA/PVP–xLa^{3+} composite polymer films are shown in Fig. 3. The spectra exhibit characteristics of various stretching and bending vibrations bands and show shift in some band positions and intensity change in others compared with the virgin polymer composite film. As noticed in Fig. 3, the FT-IR spectrum of pure PVA/PVP composite exhibits a strong broad absorption band recorded at 2837 cm^{-1}–3630 cm^{-1}, which attributed to the hydroxyl (O–H) stretching vibration [3, 4, 38]. This band gets

Table 1 The structural parameters of PVA/PVP and PVA/PVP–xLa^{3+} polymer composite

Sample	2θ (°)	β (Rads.)	d (nm)	D (nm)	R(nm)	I/I_o %
A	19.73	0.129	0.449	1.139	0.562	100
B	20.08	0.083	0.442	1.772	0.552	44.24
C	20.52	0.076	0.432	1.936	0.540	37.49
D	20.25	0.082	0.438	1.794	0.547	37.30
E	20.05	0.073	0.442	2.015	0.552	31.13

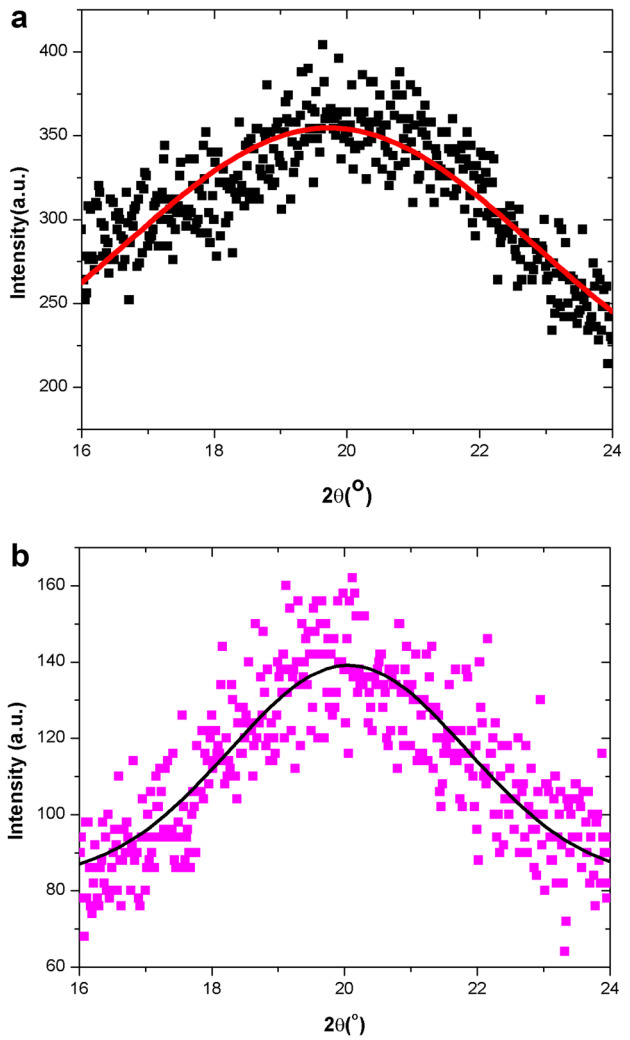

Fig. 2 Gaussian fitting of (101) XRD peak for **a** pure PVA/PVP and **b** PVA/PVP–15wt% La^{3+} polymer composite films

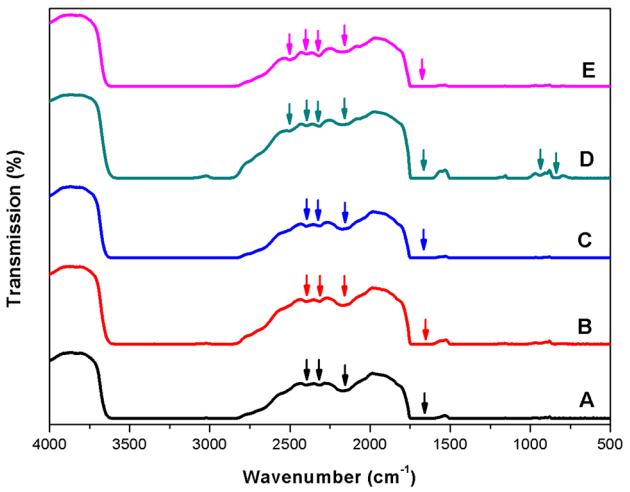

Fig. 3 FT-IR spectra of PVA/PVP–$x$$La^{3+}$ polymer composite films

shifted to 3609 cm^{-1}–2837 cm^{-1}, 3609 cm^{-1}–2844 cm^{-1}, 3593 cm^{-1}–2846 cm^{-1}, and 3615 cm^{-1}–2849 cm^{-1} in the FT-IR spectra of A, B, C, D, and E composite polymer films. The observed shift in wave numbers suggests the interaction of La^{3+} dopants with the host polymer which confirmed by the XRD measurements. In addition to this broad peak, several characteristic absorption bands observed at about 2394 cm^{-1}, 2321 cm^{-1}, and 2157 cm^{-1} were observed for all film samples. These bands may assigned to C≡O, C≡C, and C≡N stretching vibration, respectively [3, 4], and they exhibit change in intensity by increasing the doping level of La^{3+} ions in the (PVA/PVP) composite matrix due to replacement of carbon atoms with lanthanum in the chains of the polymer composite.

3.3 Optical properties

In particular, it has been established that measuring the optical absorption is a potential technique useful in the elucidation of the optical characteristics and determining various optical parameters such as absorption edge, optical gap, and refractive index of crystalline and amorphous materials.

3.3.1 Optical absorption studies

The UV–visible transmission and absorption spectra of PVA/PVP and PVA/PVP–$x$$La^{3+}$ are shown in Fig. 4a and b. The results indicate that PVA/PVP strongly blocks UV radiations and the blocking range is progressively increased from (200–230 nm) for pure VA/PVP composite film to (200–240 nm) for PVA/PVP–15wt% La^{3+} (see inset of Fig. 4). It is noticed that there is a significant shift in absorption band edges towards the higher wavelengths and this shift increases by increasing La^{3+} ions content in PVA/PVP chains. The shifting in the absorption edge may attribute to the change in the structure parameters due to complexation of La^{3+} ions in the polymer composite which results in the formation of intra/intermolecular bonding between La^{3+} ions with the adjacent carbonyl groups of PVA/PVP in the polymer composite chains. This result confirms the obtained results of the XRD analysis. An absorption band was observed at about 286 nm, whereas pure composite can be assigned to n–π* [39] transitions and the intensity of this band increases with increase in La^{3+} concentration in the composite films. The rise in absorption band is due to enrichment to the number of absorbing molecules in the sample due to the inter-/intra molecular hydrogen bonding between the carbonyl group of PVP and the hydroxyl group of PVA and La^{3+}. Although the transmission decreases gradually by increasing La^{3+} content in the composite in the visible range, there are no detected absorption bands in this range. This

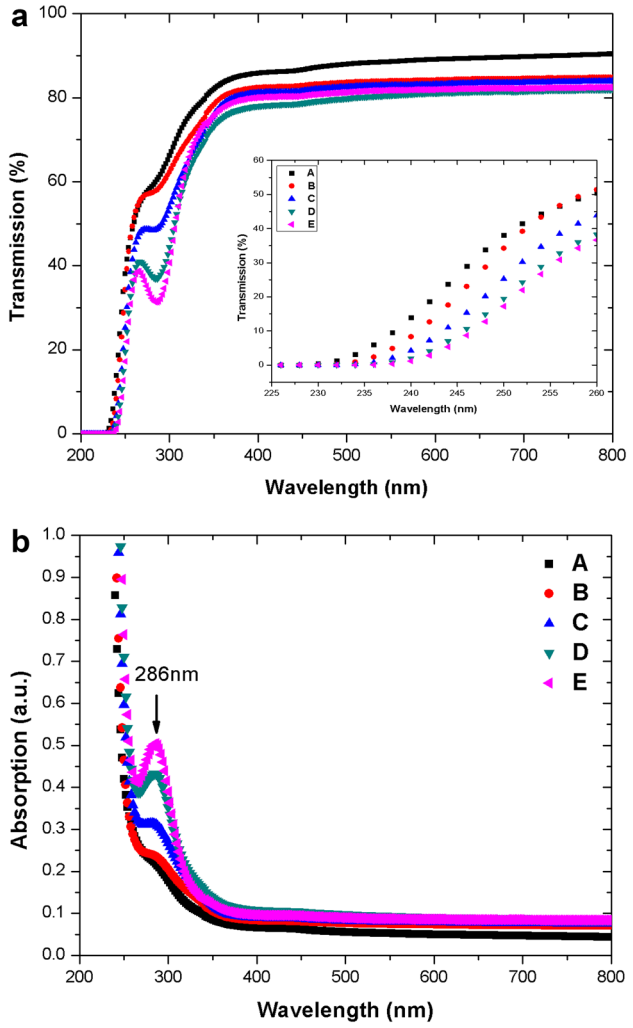

Fig. 4 **a** Optical transmission spectra and **b** optical absorption spectra of PVA/PVP–xxLa^{3+} polymer composite films

result explains the transparency and colorlessness of the sample to the human eyes. For better comparison of the optical properties, the absorption of light by an optical medium is quantified by its absorption coefficient $\alpha(\lambda)$ because it is independent on the thickness of the sample. The absorption coefficient $\alpha(\lambda)$ is defined from the optical density (O.D.) that is sometimes called absorption $A(\lambda)$ as O.D. $= 0.434\alpha l$, where l is the thickness and O.D. $= -\log T$. The relation between the absorption coefficient α and photon energy $h\nu$ for PVA/PVP–La^{3+} composite films is shown in Fig. 5. The absorption edge of the films can be determined from extrapolating the linear segment to zero absorption value. An observable decrease in the values of the absorption edge for PVA/PVP–La^{3+} composite was detected as La^{3+}wt% increases, which indicates the augmentation of the compositional disorder and formation of some localized states in the band gap [40–42].

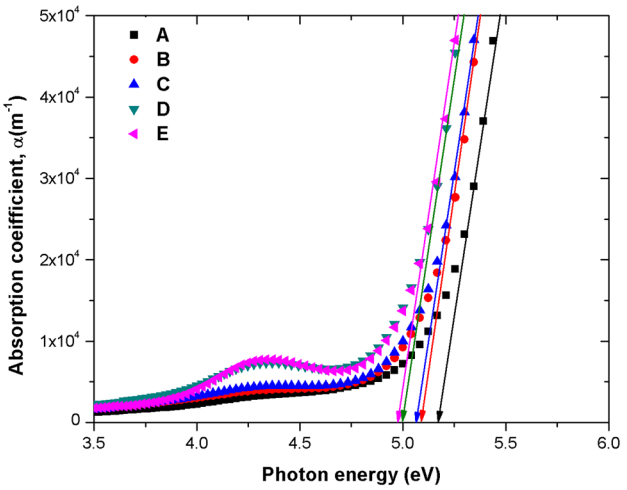

Fig. 5 Plot of the absorption coefficient (α) versus photon energy ($h\nu$) for PVA/PVP–xLa^{3+} polymer composite films

3.3.2 Optical band gap determination

The optical transition, optical band gap, and band structure of various materials can be determined using the interband absorption model [43]. According to this model, a photon can be exciting an electron from the top of the valance band to an unoccupied state at the bottom of the conduction band. Particularly, measurements of the optical absorption near the fundamental absorption edge are the most widespread methods for the investigation of optically induced electronic transition in many solid materials. The optical energy gap E_g of the composite films can be calculated using various models such as Tauc [3, 4, 36, 38–42], absorption spectra fitting [4, 44–46], and optical dielectric loss [47, 48] which produce closely equal values [49, 50]. The general expression of Tauc's, Davis, and Mott [38–42] is one of the most important parameters that can be explained the optical and electrical features of insulators and semiconductors. An accurate value of the band gap is needed because it controls the application of the material.

3.3.2.1 (a) Tauc's method Tauc relation is widely used to determine the band gap from optical absorption coefficient α as a function of photon energy $h\nu$ according to

$$(\alpha h\nu)^m = C\left(h\nu - E_g\right), \tag{4}$$

where C is the proportionality constant and m is a power factor describing the kind of electronic transition from the valance band to the conduction band which responsible for absorption. For indirect allowed transition the factor $m = 1/2$ and for indirect allowed transition $m = 2$. One can notice from Fig. 5 that the films exhibit strong absorption at short wavelength region indicating the increase of the probability

of allowed indirect transition. The indirect band gap can estimated from the extrapolation of the linear segment of $(\alpha h\nu)^{\frac{1}{2}}$ versus $h\nu$ relation to zero absorption coefficient ($\alpha = 0$) as shown in Fig. 6. It is observed that the band gap of pure PVA/PVP composite is about 4.88 eV in a good agreement with the previous published work [3, 4, 39] and slightly reduced by increasing La^{3+} ions contents in the composite chains to reach to 4.75 eV for PVA/PVP–15wt% La^{3+}. This result considers a confirmation of incorporation of La^{3+} ions to the PVA/PVP matrix and indicates augmentation of the amorphicity of the PVA/PVP–xLa^{3+} composite polymer films.

3.3.2.2 (b) Absorption spectra (ASF) fitting procedure In fact to get an accurate value of optical band gap using Tauc's relation, it is necessary to measure the sample thickness precisely which sometimes not possible for small thickness polymer film. Therefore, a more accurate method to find the optical gap was proposed [51–55]. This method is known as absorption spectra fitting and abbreviated as (ASF). In ASF method, the optical band gap can be calculated directly from absorbance (A) data only avoiding the thickness film measurement. According to this method, the optical gap can be determined from the following relation [51–55]:

$$A(\lambda) = D_1 \lambda \left(\frac{1}{\lambda} - \frac{1}{\lambda_g} \right)^m + D_2, \quad (5)$$

where D_1 and D_2 are constants, and λ_g is the band gap wavelength. The indirect optical band gap can be determined from extrapolation of the linear segment of $\left(\frac{A(\lambda)}{\lambda}\right)^{\frac{1}{2}}$ versus $\left(\frac{1}{\lambda}\right)$ relation as shown in Fig. 7. Then,

$$E_g^{ASF} = \frac{1239.83}{\lambda_g} (\text{ev})$$

The variation of the indirect band gap (E_g) determined by Tauc and ASF method is presented in Fig. 8. Comparing Figs. 6 and 7 and 8 one can notice that the decrease in optical band gap is more obvious using the ASF method and the optical gap of pure PVA/PVP composite is 4.79 eV and reduces to 4.62 eV for PVA/PVP–15wt% La^{3+}. This small difference between the values of the band gaps determined from Tauc and ASF methods may be assigned to the less precision measurement of the sample thickness used in Tauc's relation which is totally avoided in all calculations using ASF method.

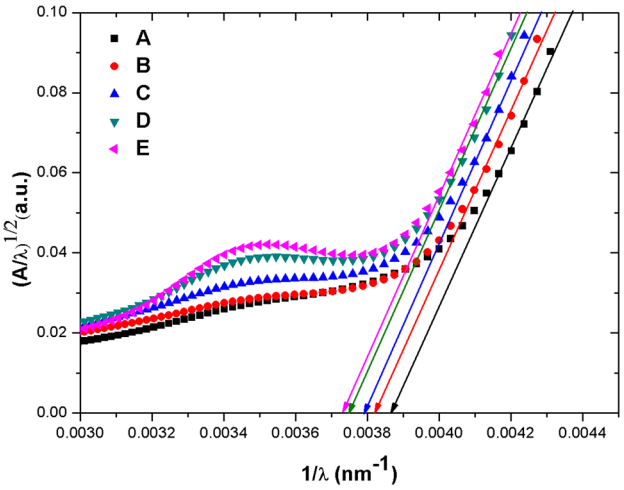

Fig. 7 Plots of $(A/\lambda)^{1/2}$ versus (l/λ) for (PVA/PVP)–xLa^{3+} polymer composite films

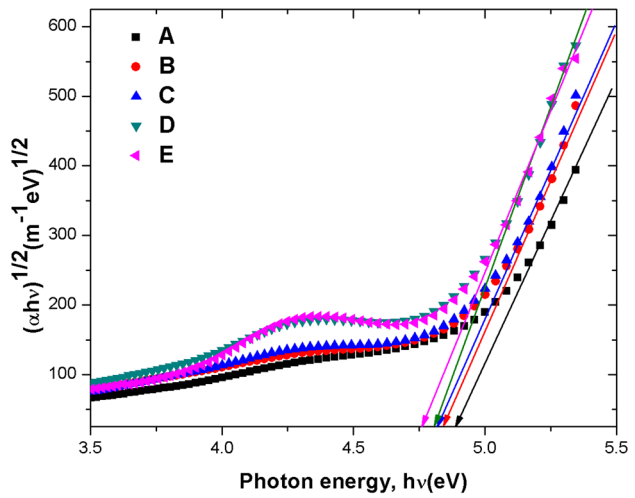

Fig. 6 Plots of $(\alpha h\nu)^{1/2}$ versus $(h\nu)$ for (PVA/PVP)–xLa^{3+} polymer composite films

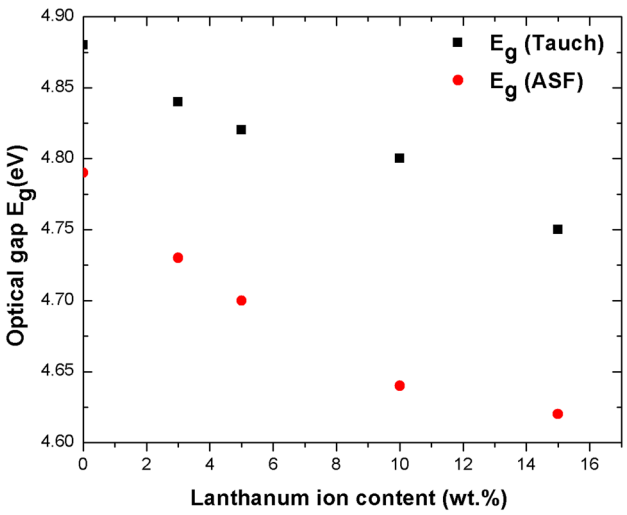

Fig. 8 Dependence of the indirect optical gap $E_{g\text{-ind.}}$ on La^{3+} ions concentration based on Tauc's and ASF methods

3.3.3 Refractive index

The refractive index is an uniquely important parameter of optical materials that determines the optical characteristics of a material. Thus, controlling the refractive index of optical materials is needed for different applications extended from protective coating to the designing of solid state lasers [56–60]. There are various empirical relations that can be used to determine the high-frequency refractive index from the band gap of the material [56, 57], and among them, the relation proposed by Dimitrov et al. [58];

$$\left(\frac{n^2-1}{n^2+2}\right) = 1 - \left(\frac{E_g}{20}\right)^{\frac{1}{2}} \quad (6)$$

was successfully used to determine the high refractive index of the polymer films.

Based on this relation, the refractive indices values for PVA/PVP–xLa^{3+} composite polymer films were calculated from the optical gap determined by the ASF method and collected in Table 2. It is discerned from Table 2 that the refractive index of PVA/PVP–xLa^{3+} composite polymer films increases gradually and very slightly from 1.757 for pure PVA/PVP to 1.777 for PVA/PVP–3La^{3+} composite film sample. Although the change in refractive index is very small, such variation in refractive index is important and desirable in the fabrication of polymer waveguides in which the refractive index of the core is slightly higher than that of the cladding to insure propagation of light through the core by total internal reflection. These results may be attributed to the increase in the density of PVA/PVP–xLa^{3+} composite films due complexation of La^{3+} in the polymer matrix. This result was also confirmed in XRD parameters measurements where the inter-chain separation also slightly decreases which reflects the more compact of the composite chains and lamellae of the polymer composite and thereby increasing the density of the final product.

Table 2 Fundamental absorption edge (E_{edge}), Optical gap (E_g) and high-frequency refractive index (n) of PVA/PVP–xLa^{3+}composite films

Sample	E_{edge} (e.V)	$E_g^{(T)}$(e.V)	$E_g^{(ASF)}$(eV)	$n_{Dim.}^{(ASF)}$
A	5.16	4.88	4.79	1.757
B	5.07	4.84	4.73	1.764
C	5.05	4.82	4.70	1.767
D	4.99	4.80	4.64	1.775
E	4.96	4.75	4.62	1.777

3.4 Electrical properties

The dielectric parameter (ε') and dielectric loss (ε'') represent energy storage and energy loss of AC external electric field. Figure 9a, b shows the frequency dependence of both ε' and ε'' of the [(PVA/PVP)–xLa^{3+}] composite polymer films at room temperature. It is clear from Fig. 9a that the dielectric parameter ε' versus frequency (f) reflects the influence of La^{3+} ions content on the characterization of pure PVA/PVP composite films. High values of ε' and ε'' were produced in pure PVA/PVP composite films, and they tend to decrease by increasing La^{3+} ions content in the PVA/PVP composite films. This behavior can be explained on the basis of decreasing electrical polarization due to decreasing directional polarization (dipole response) and ionic polarization (elongation and shrinkage of bonds between ions) in the PVA/PVP polymer composite films with the external electric field due to increasing La^{3+} ions content. This in turn depends on the large mass of La^{3+}ions and its bond strength in the polymer chain where it replaces carbon atoms as mentioned before in the FT-IR analysis. Hence,

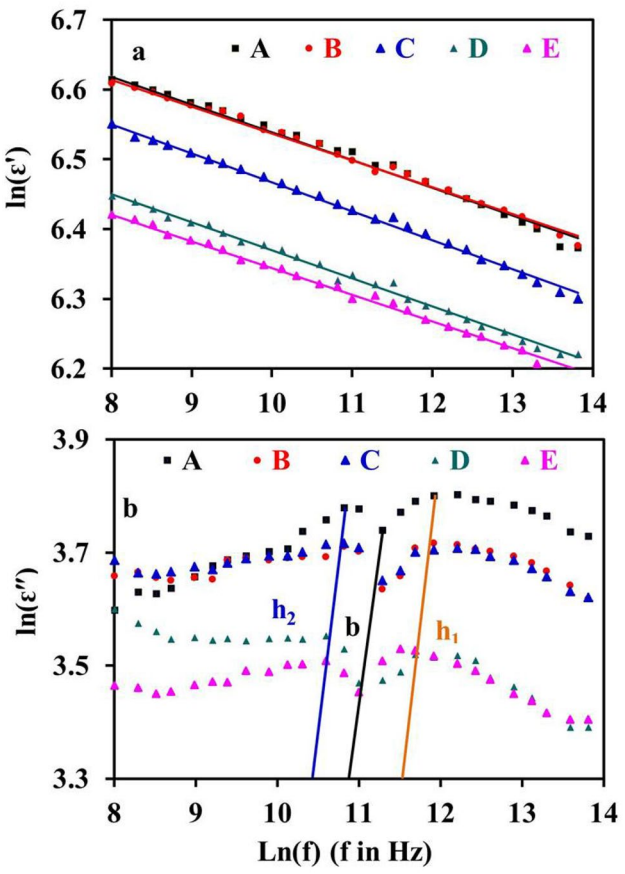

Fig. 9 Frequency dependence of **a** dielectric parameter (ε') and **b** dielectric loss (ε'') of (PVA/PVP)–xLa^{3+}polymer composite films at room temperature

it can be associated to the inability of electrical dipoles to rotate rapidly leading to a lag between the oscillating AC electrical fields and oscillating frequency of the electrical dipoles of the investigated samples. In addition, the bond length decreases (force constant increases) due to the decrease in the inter-planar spacing (d) and the average crystallite separation (R) with the increase of La ions content in the PVA/PVP polymer composite films as shown in Table 1. This means that the distance between La ions is reduced, and subsequent increase in the interaction between them, which may reduce the dipole–dipole interaction (i.e., a reduction in ε') [61, 62]. From this point of view, ε' of the pure PVA/PVP polymer will be higher than that of the doping polymers. Figure 9 shows that decreasing ε' with increasing frequency (as a normal behavior for these materials) that may be due to decreasing the rotational dipoles, interfacial and accumulation polarizations of the samples which can follow the high ac external filed on according to the mechanism of polarization [63]. It is observed from Fig. 9b that ε'' spectra with frequency have two humps (at average values $\overline{h}_1 \approx 125$ kHz and at $\overline{h}_2 \approx 45$ kHz) and one bottom (at average value $\overline{b} \approx 70$ kHz). The appearance of the humps in the dielectric loss spectra suggests the presence of relaxing dipoles in the polymer film. The strength of the relaxation depends on the characteristic property of dipolar relaxation. So, the first ($\overline{h}_1$) and second humps ($\overline{h}_2$) correspond to the average PVA polymer ions polarization relaxation frequency ($\overline{f}_1$) (the average shorter relaxation time [36, 37], $\overline{\tau}_1 = 1.274 \times 10^{-06}$ s) and the average PVP polymer ions polarization relaxation frequency ($\overline{f}_2$) (the average longer relaxation time [64], $\overline{\tau}_2 = 3.539 \times 10^{-6}$ s). The shift of h_1 and h_2 positions to lower frequencies (longer relaxation time) indicates that lanthanum cations prefer to coexist with the PVA polymer chains by replacing carbon atoms and bonding with anions. The bottom (b) on ε'' spectra may be attributed to PVA/PVP interfaces of average polarization relaxation frequency ($\overline{f}_3$). At the lower frequency, the minimum energy loss is occurred, so these materials may be selected to be used in energy applications.

Figure 10 presents the frequency-dependent AC electrical conductivity (σ_{AC}) of PVA/PVP–xLa^{3+} composite polymer films at room temperature. It is also noticed from this Figure that σ_{AC} is found to be higher for pure PVA/PVP films compared to doping of PVA/PVP films and it decreases with increasing doping of PVA/PVP films with La ions. The mobility (vibration) of ions in polymers chains is restricted with increasing La^{3+} ions content as a result to heavy mass of La ions as compared to carbon ions and this leads to reduction of AC electrical conductivity.

I–V characteristics of the fabricated PVA/PVP–xLa^{3+} composite polymer films at room temperature are shown in Fig. 11. I–V curves show a linear-like ohmic behavior. This ohmic character of these samples means that La ions are

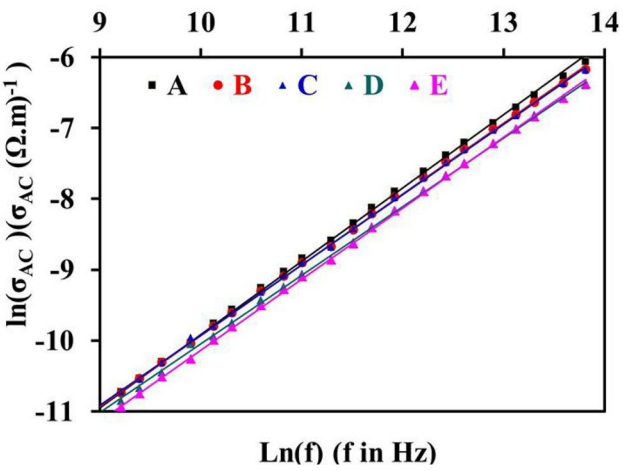

Fig. 10 ln(σ_{AC}) versus ln (f) of (PVA/PVP)–xLa^{3+} polymer composite films at room temperature

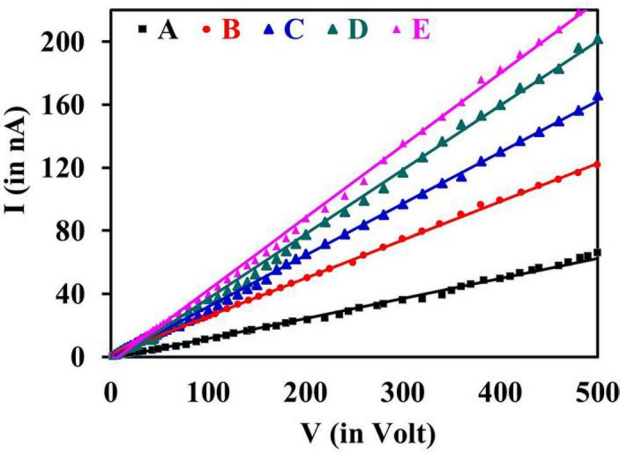

Fig. 11 I–V characterization of (PVA/PVP)–xLa^{3+} polymer composite films at room temperature

bonded well in the structure of polymers and became part of it. Variation of ρ_{DC} depends on La^{3+} ions content where the resistivity increases with the increasing La ions content. The values of resistivity (ρ_{DC}) lie in the range 5.5×10^7 Ω.m. to 2×10^6 Ω.m. These high resistivity values of these materials make them candidates for high-frequency applications.

4 Conclusion

High-quality and low-cost PVA/PVP–La^{3+} composite films have been prepared using the simple and conventional casting technique. The complexation of La^{3+} ions in the PVA/PVP polymer blend was confirmed from the obtained results of the XRD structural parameters and FT-IR spectra. The optical gaps of PVA/PVP–La^{3+}

determined from Tauc's relation and the ASF method, $E_g^{(T)}$ and $E_g^{(ASF)}$ are nearly equal and exhibit a decreasing trend with increasing La^{3+} contents. The high-frequency refractive index calculated from the optical gap values exhibit a small increase with increasing La^{3+} ions in the polymer composite. As a result of La^{3+} doping, a significant decrease in directional and ionic polarization of PVA/PVP blend films was observed resulting in a decrease of the dielectric constants ε' and ε''. The minimum energy loss of the film samples occurred at 70 kHz and the I–V characteristics show a linear-like ohmic behavior. These materials may be selected to use in energy applications. In view of the collected data, it could be suggested that PVA/PVP–xLa^{3+} polymer composite films are expected to be a novel interesting optical material possessing great potential and significant importance for multifunctional applications as polymer planar waveguide and energy devices for various display applications.

References

1. S.A. Stepanchikova, R.P. Biteykina, A.A. Sava, An experimental study of hydrolytic behavior of thulium in basic and near-neutral solutions. Open J. Inorg. Chem. **3**(2), 42–47 (2013)
2. T.A. Hamdalla, T.A. Hanafy, A.E. Bekheet, Influence of erbium ions on the optical and structural properties of polyvinyl alcohol. J. Spectrosc. (2015). https://doi.org/10.1155/2015/204867
3. F.M. Ali, R.M. Kershi, M.A. Sayed, Y.M. AbouDeif, Evaluation of structural and optical properties of Ce^{3+} ions doped (PVA/PVP) composite films for new organic semiconductors. Phys. B **538**, 160–166 (2018)
4. F.M. Ali, Structural and optical characterization of [(PVA:PVP)-Cu2 +] composite films for promising semiconducting polymer devices. J. Mol. Struct. **1189**, 352–359 (2019)
5. O.G. Abdullah, S.B. Aziz, M.A. Rasheed, Structural and optical characterization of PVA: $KMnO_4$ based solid polymer electrolyte. Results Phys. **6**, 1103–1108 (2016)
6. H.M. Zidan, N.A. El-Ghamaz, A.M. Abdelghany, A. Lotfy, Structural and electrical properties of PVA/PVP composite doped with methylene blue dye. Int. J. Electrochem. Sci. **11**, 9041–9905 (2016)
7. M. Banerjee, A. Jain, G.S. Mukherjee, Microstructural and optical properties of polyvinyl alcohol/manganese chloride composite film. Polym. Compos. **40**, E765–E775 (2019)
8. J.P. Sharma, P. Kumar, Optical and luminescence study of PVP/PPO membranes. Int. J. New. Hor. Phys. **2**(2), 95–97 (2015)
9. H.M. Zidan, E.M. Abdelrazek, A.M. Abdelghany, A.E. Tarabiah, Characterization and some physical studies of PVA/PVP filled with MWCNTs. J. Mater. Res. Technol. **8**(1), 904–913 (2019)
10. B.M. Baraker, B. Lobo, Experimental study of PVA-PVP composite films doped with cadmium chloride monohydrate. Indian J. Pure Appl. Phys. **54**, 634–640 (2016)
11. S. El-Gamal, M. El Sayed, Physical properties of the organic polymeric composite (PVA/PAM) modified with MgO nanofillers. J. Compos. Mater. **53**(20), 2831–2847 (2019)
12. M.M. El-Desoky, M. Morad, M.H. Wasfy, A.F. Mansour, Structural and optical properties of TiO_2/PVA nanocomposites. IOSR J. Appl. Phys. (IOSR-JAP) **9**(5), 33–43 (2017)
13. O.G. Abdullah, Y.A.K. Salman, S.A. Saleem, In-situ synthesis of PVA/HgS nanocomposite films and tuning optical properties. Phys. Mater. Chem. **3**(2), 18–24 (2015)
14. H.M. Ragab, Studies on the thermal and electrical properties of polyethylene oxide/polyvinyl alcohol composite by incorporating of cesium chloride. Results Phys. **7**, 2057–2065 (2017)
15. R.J. Sengwa, S. Choudhary, Nonlinear enhancement of the dielectric properties of PVA-Al_2O_3 nanocomposites. Adv. Mater. Proc. **2**(4), 280–287 (2017)
16. T. Fahmy, A. Sarhan, I.A. Elsayed, M.T. Ahmed, Effect of UV irradiation on the structure and optical properties of PVA/$CuCl_2$. J. Adv. Phys. **14**(2), 5378–5387 (2018)
17. B. Karthikeyan, S. Hariharan, R.V. Mangalaraja, T. Pandiyarajan, R. Udayabhaskar, P. Sreekanth, Studies on NiO-PVA composite films for opto-electronics and optical limiters. IEEE Photon. Technol. Lett. **30**(17), 1539–1542 (2018)
18. E.M. Abdelrazek, H.M. Ragab, Spectroscopic and dielectric study of iodine chloride doped PVA/PVP composite. Indian J. Phys. **89**(6), 577–585 (2015)
19. Houssein Awad, Claude Daneault, Chemical modification of poly(Vinyl Alcohol) in water. Appl. Sci. **5**, 840–850 (2015)
20. E.M. Abdelrazek, I.S. Elashmawi, A. El-khodary, A. Yassin, Structural, optical, thermal and electrical studies on PVA/PVP composite s filled with lithium bromide. Curr. Appl. Phys. **10**, 607–613 (2010)
21. J. Qiao, J. Fu, R. Lin, J. Ma, J. Liu, Alkaline solid polymer electrolyte membranes based on structurally modified PVA/PVP with improved alkali stability. Polymer **51**, 4850–4859 (2010)
22. D.R. Raj, S. Prasanth, T.V. Vineeshkumar, C. Sudarsanakumar, Ammonia sensing properties of tapered plastic optical fiber coated with silver nanoparticles/PVP/PVAhybrid. Opt. Commun. **340**, 86–92 (2015)
23. E.M. Abdelrazek, I.S. Elashmawi, S. Labeeb, Chitosan filler effects on the experimental characterization, spectroscopic investigation and thermal studies of PVA/PVP composite films. Phys. B **405**, 2021–2027 (2010)
24. Yan Shi, Dangsheng Xiong, Jinfeng Zhang, Effect of irradiation dose on mechanical and bio tribological properties of PVA/PVP hydrogels as articular cartilage. Tribol. Int. **78**, 60–67 (2014)
25. W.H. Eisa, Y.K. Abdel-Moneam, A.A. Shabaka, A.E. Hosam, In situ approach induced growth of highly mono dispersed Ag nanoparticles within free standing PVA/PVP films. Spectrochim. Acta, Part A **95**, 341–346 (2012)
26. Yan Shi, Dangsheng Xiong, Microstructure and friction properties of PVA/PVP hydrogels for articular cartilage repair as function of polymerization degree and polymer concentration. Wear **305**, 280–285 (2013)
27. Ruyin Ma, Dangsheng Xiong, Feng Miao, Jinfeng Zhang, Yan Peng, Novel PVP/PVA hydrogels for articular cartilage replacement. Mater. Sci. Eng., C **29**, 1979–1983 (2009)
28. T.A. Hamdalla, T.A. Hanafy, Optical properties studies for PVA/Gd, La, Er or Y chlorides based onstructural modification. Optik **127**, 878–882 (2016)
29. V.S. Smitha, P. Saju, U.S. Hareesh, G. Swapankumar, K.G.K. Warrier, Optical properties of rare-earth doped tio$_2$ nanocomposites and coatings; a sol-gel strategy towards multi–functionality. Chem. Sel. **1**, 2140–2147 (2016)
30. M.O. Reddy, B.C. Babu, Structural, optical, electrical, and magnetic properties of PVA:Gd^{3+} and PVA:Ho^{3+} polymer films. Indian J. Mater. Sci. **2015**, 1–8 (2015)
31. B. Kumar, G. Kaur, S.B. Rai, Sensitized green emission of terbium with dibenzoylmethane and 1, 10 phenanthroline in polyvinyl alcohol and polyvinyl pyrrolidone composites. Spectrochim. Acta, Part A **187**, 75–81 (2017)
32. H. Ma, T. Shi, Q. Song, Synthesis and characterization of novel PVA/SiO_2-TiO_2 hybrid fibers. Fibers **2**, 275–284 (2014)

33. D.W. Chae, Y.W. Kim, E.J. Lee, B.C. Kim, Effects of swelling conditions on the superstructure of PVA films during the wet drawing process. Text. Sci. Eng. **53**, 165–170 (2016)
34. S. Kumaraswamy, G. Babaladimath, V. Badalamoole, S.H. Mallaiah, Gamma irradiation synthesis and in vitro drug release studies of ZnO/PVA hydrogel nanocomposites. Adv. Mater. Lett. **8**(1), 02–07 (2017)
35. I.S. Elashmawi, A.A. Menazeab, Different time's Nd:YAG laser-irradiated PVA/Ag nanocomposites: structural, optical, and electrical characterization. J. Mater. Res. Technol. **8**(2), 1944–1951 (2019)
36. F.M. Ali, F. Maiz, Structural, optical and AFM characterization of PVA:La^{3+} polymer films. Phys. B **530**, 19–23 (2018)
37. M. Aslam, M.A. Kalyar, Z.A. Raza, Fabrication of reduced graphene oxide nanosheets doped PVA composite films for tailoring their opto-mechanical properties. Appl. Phys. A **123**(6), 424 (2017)
38. S.B. Aziz, M.A. Rasheed, A.M. Husseina, H.M. Ahmed, Fabrication of polymer composite composites based on [PVA-PVP] (1-*x*):$(Ag_2S)_x$ ($0.01 \leq x \leq 0.03$) with small optical band gaps: structural and optical properties. Mater. Sci. Semicond. Process. **71**, 197–203 (2017)
39. H.M. Zidan, N.A. El-Ghamaz, A.M. Abdelghany, A.L. Waly, Photodegradation of methylene blue with PVA/PVP composite under UV light irradiation. Spectrochim. Acta, Part A **199**, 220–227 (2018)
40. A.H. El-Sayed, Y. Hossien, M.A. Hamad, Tailoring optical transmittance of polyvinyl alcohol by $FeCl_3$-doping for photovoltaic application. Eur. Phys. J. Plus **134**, 415 (2019). **1-7**
41. O. Pravakar, T. Siddaiah, N.O. Gopal, C. Ramu, Structural, optical and electrical conductivity studies of Mn^{2+} ions doped PVA/MAA: EA polymer composite film. Int. J. Sci. Res. Phys. Appl. Sci. **6**(6), 80–87 (2018)
42. M.A. Brza, S.B. Aziz, H. Anuar, M.H.F. Hazza, From green remediation to polymer hybrid fabrication with improved optical band gaps. Int. J. Mol. Sci. **20**, 3910 (2019)
43. M.E. Sánchez-Vergara, J.C. Alonso-Huitron, A. Rodriguez-Gómez, J.N. Reider-Burstin, Determination of the optical GAP in thin films of amorphous dilithium phthalocyanine using the tauc and cody models. Molecules **17**, 10000–10013 (2012)
44. F.M. Ali, Synthesis and characterization of a novel erbium doped poly(vinyl alcohol) films for multifunctional optical materials. J. Inorg. Organometall. Polym. Mater. (2019). https://doi.org/10.1007/s10904-019-01386-8
45. L. Escobar-Alarcon, A. Arrieta, E. Camps, S. Muhl, S. Rodil, E. Vigueras-Santiago, An alternative procedure for the determination of the optical band gapand thickness of amorphous carbon nitride thin films. Appl. Surf. Sci. **254**, 412–415 (2007)
46. N. Ghobadi, Band gap determination using absorption spectrum fitting procedure. Int. Nano Lett. **3**, 2 (2013)
47. S.B. Aziz, Modifying poly(Vinyl Alcohol) (PVA) from insulator to smallbandgap polymer: a novel approach for organic solar cells and optoelectronic devices. J. Electron. Mater. **45**(1), 736–745 (2016)
48. S.B. Aziz, M.A. Rasheed, H.M. Ahmed, Synthesis of polymer nanocomposites based on [methyl cellulose](1–x):(CuS)x ($0.02\ M \leq x \leq 0.08\ M$) with desired optical band gaps. Polymers **9**(149), 1–16 (2017)
49. S.B. Aziz, S.M. Mamand, S.R. Saed, R.M. Abdullah, S.A. Hussein, New method for the development of plasmonic metal-semiconductor interface layer: polymer composites with reduced energy band gap. J. Nanomater (2017). https://doi.org/10.1155/2017/8140693
50. S.B. Aziz, Morphological and optical characteristics of chitosan(1–x): Cuo x ($4 \leq x \leq 12$) based polymer nano-composites: optical dielectric loss as an alternative method for Tauc's model. Nanomaterials **7**(444), 1–15 (2017)
51. S. Yadav, P.K. Bajpai, Effect of substrate on CuS/PVA nanocomposite thin films deposited on glass and silicon substrate. Soft Nanosci. Lett. **8**, 9–19 (2018)
52. N. Ghobadi, Band gap determination using absorption spectrum fitting procedure. Int. Nano Lett. **3**(2), 1–4 (2013)
53. Y.S. Rammah, Gamma radiation induced modification on optical gap of polycarbonate detectors. Am. J. Opt. Photon. **5**(3), 24–29 (2017)
54. K.M. Kaky, G. Lakshminarayana, S.O. Baki, Y.H. Taufiq-Yap, I.V. Kityk, M.A. Mahdi, Structural, thermal, and optical analysis of zinc boro-aluminosilicate glasses containing different alkali and alkaline modifier ions. J. Non-Cryst. Solids **456**, 55–63 (2017)
55. Y.S. Rammah, A.R. El-Sersy, I.A. El-Mesady, F.I. El-Agawany, Modifications of structural, optical, and carbonaceous clusters in neutron irradiated $C_{12}H_{18}O_7$ polymeric detector. J. Radiat. Nucl. Appl. **4**(2), 91–100 (2019)
56. R.S. Indolia, Relationship of refractive index with optical energy gap and average energy gap for II-VI and III-V group of semiconductors. Int. J. Pure Appl. Phys. **13**(2), 185–191 (2017)
57. N.M. Ravindra, P. Ganapathy, J. Choi, Energy gap–refractive index relations in semiconductors–An overview. Infrared Phys. Technol. **50**, 21–29 (2007)
58. V. Dimitrov, T. Komatsu, An interpreatation of optical properties of oxides and oxide glasses in terms of the electronic ion polarizability and average single bond strength (review). J. Univ. Chem. Technol. Metall. **45**(3), 219–250 (2010)
59. E. Keaney, J. Shearer, A. Panwar, J. Mead, Refractive index matching for high light transmission composite systems. J. Compos. Mater. **52**(24), 3299–3307 (2018)
60. N. Sultanova, S. Kasarova, I. Nikolov, Dispersion properties of optical polymers. Acta Phys. Pol., A **16**(4), 585–587 (2009)
61. S.B. Qadri, E.F. Skelton, D. Hsu, A.D. Dinsmore, J. Yang, B.R. Ratna, Size- induced transition-temperature reduction in nanoparticles of ZnS. Phys. Rev. B **60**, 9191–9193 (1999)
62. P. Vasudevan, S. Thomas, K.V. Arunkumar, S. Karthika, N.V. Unnikrishnan, Synthesis and dielectric studies of poly (vinyl pyrrolidone)/titanium dioxide nanocomposites. IOP Mater. Sci. Eng. (ICMST) **73**, 1–4 (2015)
63. M. Prabu, S. Selvesekarpanddian, A.R. Kulkarni, S. Karthikeyan, G.S. Hiranku-mar, C. AnjeeviRaj, Ionics **17**, 201–207 (2011)
64. R.J. Sangwa, S. Sankhla, Poly(vinylepyrrolidone)-poly(ethylene glycol) composites colloid. Polym. Sci. **285**, 1237 (2007)